DOI: 10.61782/fa.2023.1195

forum acusticum 2023

MEASUREMENT BASED ABSORPTION CHARACTERISTICS ESTIMATION OF EXTENDED REACTIVE SURFACES

Gergely Firtha[1,2] **Csaba Huszty**[2]
[1] Dept. of Networked Systems and Services, Budapest University of Technologies and Economics, H-1111 Budapest, Hungary
[2] ENTEL Engineering Research & Consulting Ltd., H-1025 Budapest, Szépvölgyi út 32., Hungary

ABSTRACT

The measurement of surface impedance and the absorption/transmission characteristics is well-established for acoustic materials that can be considered locally reactive: Impedance tube-based and in-situ measurement techniques are codified in multiple ISO standards, e.g. ISO 354 and ISO 10534. However, as lateral wave propagation in the material under test becomes significant, locally reactive assumptions fail and the standardized measurement methods become infeasible. The present contribution discusses the measurement of non-locally (or extended) reactive surfaces by estimating its distributed surface impedance function and the consequent numerical prediction of the reflected sound field in a simple planar geometry. The model is validated via the measurement of a resonant panel absorber. Finally, the extension of the absorption coefficient for non-locally reactive surfaces is discussed.

Keywords: *non-locally reacting, absorption measurement, admittance measurement.*

1. INTRODUCTION

The measurement of complex surface impedances and random/oblique incident absorption coefficients of acoustic absorber materials is of great interest in the field of room acoustic design. Reverberation chamber based absorption measurement allows the estimation of the statistical random incident absorption of samples of over $10-12\mathrm{m}^2$ area, as given in ISO 354:2003 [1]. Impedance-tube and in-situ (e.g. two microphone free field measurement) measurements yield the specific impedance at a certain position on the absorber surface, from which normal incidence absorption coefficients can be calculated according to ISO 10534-2:1998 [2].

However, all the standardized impedance measurement approaches assume that the acoustical behaviour of the sample under investigation is perfectly determined by the specific impedance at the given measurement position. This approach, which completely ignores wave propagation in the absorber material or on the absorber surface, is termed as the *locally reacting surface* assumption. Certain acoustic materials, e.g. a single layer of porous absorber in certain installation circumstances can indeed be feasibly modelled as a locally reacting surface as long as the material sample is large enough to support the neglection of diffractional waves from the edges. In order to ensure this, traditional standard impedance measurement techniques require material samples with an area of over $1\ \mathrm{m}^2$.

Locally reacting assumptions fail when lateral wave propagation is significant in the test material often resulting in absorption coefficients above unity [3, 4]. These type of materials are usually referred to as *non-locally* or *extended reacting surfaces* [5]. An important example of these are plate absorbers of relatively small dimensions exhibiting strong modal behaviour on the top-plate. In these cases the pressure and the velocity at a given position are heavily influenced by the plate motion at adjacent surface positions. In order to take the coupling between

*__Corresponding author__: firtha@hit.bme.hu.

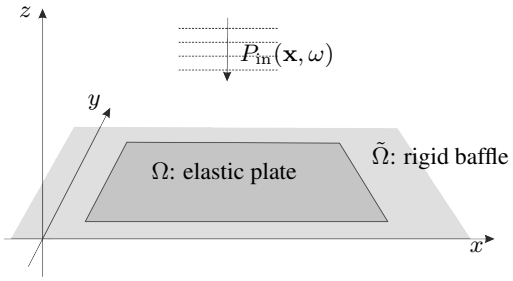

Figure 1. Geometry for scattering from an elastic plate.

the neighbouring points on the surface into consideration, multiple measurement positions are required and mutual impedances have to be estimated.

The present contribution discusses an impedance measurement method for extended reacting surfaces of small dimensions through the example of a plate resonator. The approach relies on the estimation of self- and mutual admittance over the absorber surface by means of direct mechanical admittance measurement via impact testing. The acoustic behaviour of the absorber can be predicted from the estimated admittance function for an arbitrary incident wave field, impinging on the surface of the panel. Finally, the numerical evaluation of the acoustic field on the top-plate allows the estimation of the sound absorption coefficient.

2. METHOD

2.1 Physical model for scattering from extended reactive surfaces

Assume a finite, planar extended reactive (e.g., elastic) surface, baffled into an infinite rigid plane at $z = 0$. The geometry under discussion is depicted in Fig. 1 with an exemplary rectangular plate. Points over the elastic plate are denoted by Ω, while positions on the rigid baffle are denoted by $\tilde{\Omega}$.

The plane is loaded by the infinite half-space consisting of fluid of density ρ_0 in which the speed of sound is denoted by c. The planar surface is exposed to an arbitrary steady-state incident wave field $P_{\text{in}}(\mathbf{x},\omega)$, propagating towards the elastic plate and oscillating at an angular frequency ω. As the incident wave is scattered from the surface, three main components can be identified in the resulting total pressure field:

- The incident field $P_{\text{in}}(\mathbf{x},\omega)$
- A part of the incident field that is reflected directly from the plate surface, denoted by $P_{\text{refl}}(\mathbf{x},\omega)$; and
- The pressure field on the plate surface that acts as a force distribution on the plate, generating the harmonic vibration of the surface due to its elasticity. This vibration re-radiates a sound wave into the positive half space, denoted by $P_{\text{rerad}}(\mathbf{x},\omega)$.

Thus, the total pressure field can be written as

$$P_{\text{tot}}(\mathbf{x},\omega) = P_{\text{in}}(\mathbf{x},\omega) + \underbrace{P_{\text{refl}}(\mathbf{x},\omega) + P_{\text{rerad}}(\mathbf{x},\omega)}_{P_{\text{scat}}(\mathbf{x},\omega)}. \tag{1}$$

The total scattered field (denoted by $P_{\text{scat}}(\mathbf{x},\omega)$) is, therefore, composed of the directly reflected and re-radiated field. We aim at evaluating the total field in (1) given that the equation of motion of the plate is known. For the sake of brevity we omit noting the dependence on angular frequency.

The boundary conditions can be formulated in the present geometry as follows:

- On the infinite rigid baffle the total velocity is zero. Written in terms of the pressure gradient this yields

$$\frac{\partial}{\partial z} P_{\text{in}}(\mathbf{x}) = -\frac{\partial}{\partial z} P_{\text{scat}}(\mathbf{x}) \tag{2}$$

$$P_{\text{in}}(\mathbf{x}) = P_{\text{scat}}(\mathbf{x}), \qquad \mathbf{x} \in \tilde{\Omega} \tag{3}$$

- On the elastic surface it is assumed that the transfer admittance is defined between each point, reading as

$$Y(\mathbf{x},\mathbf{x}_0) = \frac{A(\mathbf{x})}{P(\mathbf{x}_0)}, \tag{4}$$

where $A(\mathbf{x})$ is the normal acceleration of the surface at the receiver position $\mathbf{x}$, and $P(\mathbf{x}_0)$ is a point-like excitation pressure at the source position $\mathbf{x}_0$. Considering a continuous pressure distribution along the elastic surface, the corresponding acceleration is obtained as

$$A(\mathbf{x}) = \int_{\Omega} Y(\mathbf{x},\mathbf{x}_0) P(\mathbf{x}_0)\, \mathrm{d}\mathbf{x}_0. \tag{5}$$

In the present geometry the scattered field can be written in terms of a Rayleigh integral over the infinite plane $z =$

0 [6, 7], resulting in the expression for the total field at an arbitrary receiver position $\mathbf{x} = [x,\ y,\ z \geq 0]^{\mathrm{T}}$

$$P_{\mathrm{tot}}(\mathbf{x}) = P_{\mathrm{in}}(\mathbf{x}) - 2\int_{\Omega\cup\tilde{\Omega}} \frac{\partial}{\partial z} P_{\mathrm{scat}}(\mathbf{x}_0) G(\mathbf{x},\mathbf{x}_0)\mathrm{d}\mathbf{x}_0, \tag{6}$$

with the shortened notation $\frac{\partial}{\partial z}P_{\mathrm{scat}}(\mathbf{x}_0) = \frac{\partial}{\partial z}P_{\mathrm{scat}}(\mathbf{x})\big|_{\mathbf{x}=\mathbf{x}_0}$. Here G denotes the 3D Green's function

$$G(\mathbf{x},\mathbf{x}_0) = \frac{1}{4\pi}\frac{\mathrm{e}^{-\mathrm{j}\frac{\omega}{c}|\mathbf{x}-\mathbf{x}_0|}}{|\mathbf{x}-\mathbf{x}_0|} \tag{7}$$

describing the field of a point source located at $\mathbf{x}_0$, measured at $\mathbf{x}$.

Expressing $P_{\mathrm{scat}}(\mathbf{x}_0)$ as $P_{\mathrm{tot}}(\mathbf{x}_0) - P_{\mathrm{in}}(\mathbf{x}_0)$ and realizing that the integral containing $\frac{\partial}{\partial z}P_{\mathrm{in}}$ describes the reflected field from an ideal rigid infinite plane (denoted as $P_{\mathrm{refl}}^{\mathrm{rigid}}(\mathbf{x})$) yields

$$P_{\mathrm{tot}}(\mathbf{x}) = P_{\mathrm{in}}(\mathbf{x}) + P_{\mathrm{refl}}^{\mathrm{rigid}}(\mathbf{x}) - 2\int_{\Omega}\frac{\partial}{\partial z}P_{\mathrm{tot}}(\mathbf{x}_0)G(\mathbf{x},\mathbf{x}_0)\mathrm{d}\mathbf{x}_0 \tag{8}$$

[1]. Here, it was utilized that $\frac{\partial}{\partial z}P_{\mathrm{tot}}(\mathbf{x}_0)$ vanishes over $\mathbf{x}_0 \in \tilde{\Omega}$. The integral explicitly contains the three components present in the total pressure field, as discussed previously.

Finally, expressing the pressure gradient in the air by the Euler's relation $\frac{\partial}{\partial z}P(\mathbf{x}) = -\rho_0 A(\mathbf{x})$, and coupling the radiation problem with the surface by the boundary condition (5) leads to

$$P_{\mathrm{tot}}(\mathbf{x}) = P_{\mathrm{in}}(\mathbf{x}) + P_{\mathrm{refl}}^{\mathrm{rigid}}(\mathbf{x}) + 2\rho_0\int_{\Omega}\left(\int_{\Omega} Y(\mathbf{x}_0,\mathbf{x}_1)P_{\mathrm{tot}}(\mathbf{x}_1)\,\mathrm{d}\mathbf{x}_1\right)G(\mathbf{x},\mathbf{x}_0)\mathrm{d}\mathbf{x}_0, \tag{9}$$

describing the total field implicitly, at an arbitrary receiver position $\mathbf{x}$ above the horizontal plane.

Restricting the receiver position to the elastic surface the above expression simplifies to

$$P_{\mathrm{tot}}(\mathbf{x}) = 2P_{\mathrm{in}}(\mathbf{x}) + 2\rho_0\int_{\Omega}\left(\int_{\Omega} Y(\mathbf{x}_0,\mathbf{x}_1)P_{\mathrm{tot}}(\mathbf{x}_1)\,\mathrm{d}\mathbf{x}_1\right)G(\mathbf{x},\mathbf{x}_0)\mathrm{d}\mathbf{x}_0, \tag{10}$$

with $\mathbf{x} = [x,\ y,\ 0]^{\mathrm{T}}$.

[1] Note that term $P_{\mathrm{in}}(\mathbf{x}) + P_{\mathrm{refl}}^{\mathrm{rigid}}(\mathbf{x})$ is usually referred to as the *blocked pressure* in the related literature [7, 8]

2.2 Numerical solution of the integral formula

In order to solve (10) numerically the surface of the elastic plate is discretised with the centres of the elements given by $\mathbf{x}_i$, and with the area of the i-th element given by $\mathrm{d}\Omega_i$. It is assumed that the pressure and acceleration functions are constant over each surface element, with their complex amplitudes given by vectors $\mathbf{p} = P_i = P(\mathbf{x}_i)$ and $\mathbf{a} = A_i = A(\mathbf{x}_i)$. Their interconnection is given by the admittance matrix

$$\mathbf{Y} = Y_{ij} = \frac{A_i}{P_j}. \tag{11}$$

By introducing the Green's matrix

$$\mathbf{G}^{\mathrm{s}} = G_{ij}^{\mathrm{s}} = \int_{\mathrm{d}\Omega_i} G(\mathbf{x}_j,\mathbf{x}_0)\mathrm{d}\mathbf{x}_0, \quad \mathbf{x}_j = [x,\ y,\ z=0]^{\mathrm{T}} \tag{12}$$

the continuous formulation (10) can be written in discrete form, with matrix-vector notation as

$$\mathbf{p}_{\mathrm{tot}} = 2\mathbf{p}_{\mathrm{in}} + 2\rho_0\mathbf{G}^{\mathrm{s}}\mathbf{Y}\mathbf{p}_{\mathrm{tot}}. \tag{13}$$

The system of equations can be solved for the total field on the surface of the plate by evaluating

$$\mathbf{p}_{\mathrm{tot}} = 2\left(\mathbf{I} - 2\rho_0\mathbf{G}^{\mathrm{s}}\mathbf{Y}\right)^{-1}\mathbf{p}_{\mathrm{in}}. \tag{14}$$

Furthermore, the corresponding normal velocity distribution over the absorber surface is obtained from the surface pressure as

$$\mathbf{v}_{\mathrm{tot}} = \frac{1}{\mathrm{j}\omega}\mathbf{Y}\mathbf{p}_{\mathrm{tot}}. \tag{15}$$

As a summary, it was demonstrated that the planar elastic scattering problem can be solved numerically uniquely once the admittance function/matrix is defined over the elastic surface.

3. MEASUREMENT OF THE ADMITTANCE MATRIX

The previous section discussed a general numerical method for calculating the sound field on a planar elastic surface when exposed to an arbitrary incident sound field, requiring merely the admittance matrix of the surface. The present section presents a novel impact testing based measurement method for estimating the admittance matrix in case of a plate absorber. The approach is validated by comparing the predicted sound field with actual microphone measurements.

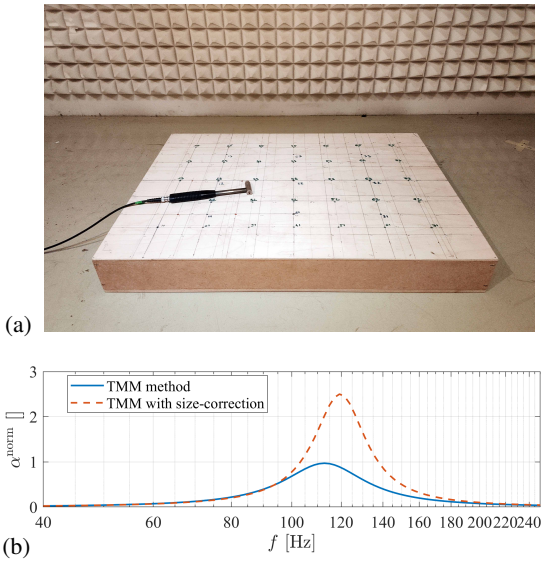

Figure 2. Plate absorber under investigation (a) and the result of TMM modeling (b).

3.1 The plate absorber under investigation

The custom built plate absorber under test is shown in Fig. 2 (a). The resonator's horizontal dimensions are $L_x = 88$ cm, $L_y = 62$ cm, meaning the total area of $\Omega = 0.55$ m^2, hence, the test object is relatively small in the aspect of absorption measurement. The construction consists of three layers:

- A composite (3-layered) plywood panel with the thickness of $t_m = 3.5$ mm, serving as the mass of the resonator structure. In accordance with the manufacturer's data sheet the mass of the plate is approximately $m_s = 2.7$ kg/m^2.
- An air gap of $d_a = 4$ cm, together with the air filling the porous absorber layer serving as the spring for the damped mass-spring absorber structure.
- A layer of rockwool $d_p = 5$ cm thick, attached to the back of the structure [2], ensuring the energy dissipation in the resonator.

[2] In the aspect of absorption efficiency the optimal choice for the position of the porous layer would be in the proximity of the plate. The present structure is non-optimal for the sake of simple construction.

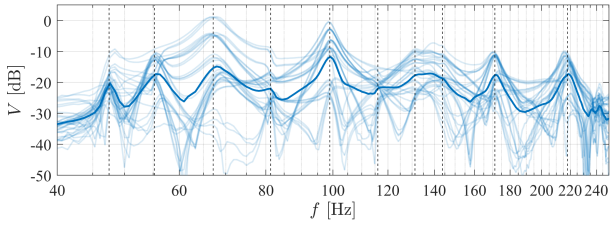

Figure 3. Velocity response along the plate surface

The backing and the framing of the structure is made out of plywood with the thickness of 1.2 cm. Overall, the simple mass-spring system based absorber was constructed to exhibit a maximal absorption at around [9]

$$f_0 = \frac{c}{2\pi}\sqrt{\frac{\rho_0}{m_s(d_p+d_a)}} = \frac{60}{\sqrt{m_s(d_p+d_a)}} \approx 121 \text{ Hz}. \tag{16}$$

As a more precise a-priori prediction for its absorption characteristics, the layered structure was modeled with the 1-dimensional transfer matrix method (TMM) [8]. The flow resistivity of the porous absorbing layer was assumed to be $\sigma_s = 45000$ rayl/m. The result of the prediction is depicted in Fig. 2 (b) in case of assuming a layered structure of infinite dimensions, and by taking the finite size into account by using a simple radiation efficiency-based correction term [8].

3.2 Impact testing of plate absorber

Section 2 highlighted that once the admittance function is known over the surface of the plate absorber, its acoustic behaviour can be numerically modelled when the layered structure is exposed to an arbitrary incident field. The admittance matrix was estimated indirectly from the results of mechanical impact testing of the resonator surface, by measuring acceleration response for an impulse like force excitation in a full grid measurement.

The measurement was carried out on a rectangular mesh by discretising the resonator surface to 7×5 points. The impact testing was performed by exciting the plate at each grid position with a PCB 086C03 impact hammer, capturing the force acting on the hammer as the excitation signal.The measured response was the normal acceleration of the grid points, measured simultaneously with five nearly identical PCB 353B13 accelerometers. The goal of the measurement was to capture the acceleration response at each receiver position a_i in case of an impulse force

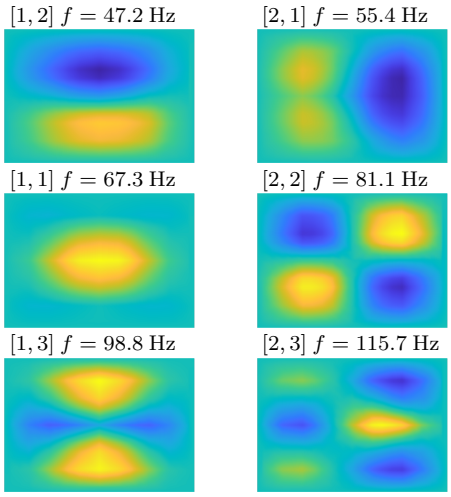

Figure 4. Mode shapes measured on the top-plate with increasing modal frequencies.

excitation at each source position f_j. The entries of the resulting acceleration matrix were obtained as the ratio of the measured acceleration and the hammer force spectra

$$\mathbf{A} = A_{ij} = \frac{a_i}{f_j}. \tag{17}$$

The number of measurements (requiring $(7 \times 5)^2 = 1225$ individual impact tests) was significantly reduced by the application of multiple accelerometers simultaneously, exploiting the reciprocity principle and assuming a symmetric plate behaviour.

The result of the measurement is depicted in Fig. 3, illustrated in terms of the plate velocity. The figure reflects that the structure under test is dominated by modal behaviour, hence the panel is strongly non-locally reacting.

Therefore, the measurement results were also subjected to experimental modal analysis in order to get an insight into the physical behaviour of the layered structure. The first six identified modes of the plate are illustrated in Fig. 4 with increasing modal frequencies. All the modes are approximately the free vibrations of the simply supported thin elastic plate, however, the order of the modes is heavily influenced by the plate's material properties and the structure of the absorber:

- For the following discussion the mode shapes are differentiated based on the number of positive and negative partitions along the surface: Modes having the same number of positive and negative cells are termed as even modes in the following, while modes with different number of positive and negative cells are referred to as odd modes (referring to the parity of the product of the modal coordinates). In case of even modes the pressure fluctuation is equalized locally behind the plate, and the acoustic short-circuit behaves as a concentrated mass connected to the back of the plate. On the other hand, in case of odd modes the air inside the enclosure has to be compressed by the plate, therefore, the cavity acts as an additional stiffness to the plate. As a result, the natural frequency of even modes slightly decreases compared to the in-vacou modes of the plate, while the frequency of odd modes (e.g. (1,1)) significantly increases.

- Furthermore, the ortotrophy of the plate leads to interchanged horizontal and vertical modal frequencies.

3.3 Calculation of the admittance matrix

So far the acceleration matrix was measured via impact testing, defining the acceleration at each surface receiver position due to a point-like force excitation at each source position. In order to arrive at the required admittance matrix the corresponding pressure field at the source position has to be evaluated for each acceleration measurement.

Written in terms of continuous velocity and pressure distribution over the absorber surface the problem can be formulated as follows: assume that the surface of the absorber is excited by a point-like force excitation at $\mathbf{x}_0$. The resulting pressure field on the surface can be divided into two main components:

- The point like pressure term being proportional to the external force excitation, described by $\delta(\mathbf{x} - \mathbf{x}_0)/\mathrm{d}\Omega(\mathbf{x}_0)$, where $\mathrm{d}\Omega(\mathbf{x}_0)$ is the area of the surface element.

- A re-radiated pressure distribution generated by the vibrating plate.

By describing the re-radiated pressure in terms of a Rayleigh integral the total pressure can be written on the

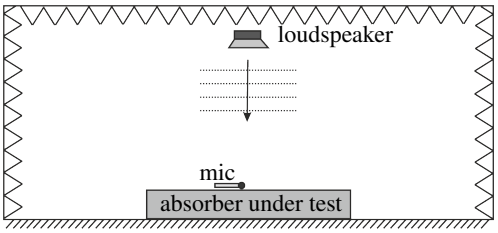

Figure 5. Measurement setup for validating the analytical and numerical results.

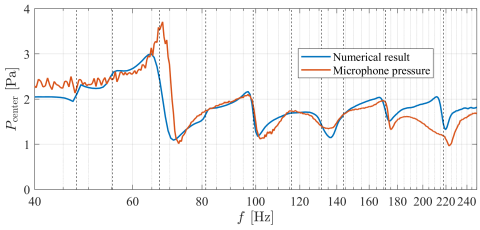

Figure 6. Pressure field at the geometrical centre of the elastic plate. Dashed vertical lines denote the estimated modal frequencies.

surface (by also applying the Euler equation) as

$$P(\mathbf{x},\mathbf{x}_0) = \frac{\delta(\mathbf{x}-\mathbf{x}_0)}{\mathrm{d}\Omega(\mathbf{x}_0)} - 2\int_\Omega \frac{\partial}{\partial z} P(\mathbf{x},\mathbf{x}_0) G(\mathbf{x},\mathbf{x}_0)\mathrm{d}\mathbf{x}_0 = \\ = \frac{\delta(\mathbf{x}-\mathbf{x}_0)}{\mathrm{d}\Omega(\mathbf{x}_0)} + 2\rho_0 \int_\Omega A(\mathbf{x},\mathbf{x}_0) G(\mathbf{x},\mathbf{x}_0)\mathrm{d}\mathbf{x}_0 \quad (18)$$

with $\mathbf{x}$ and $\mathbf{x}_0$ denoting the receiver and source positions, respectively.

The acceleration of the surface can be expressed from (5) by using the admittance function as

$$A(\mathbf{x},\mathbf{x}_0) = \left(\int_\Omega \frac{\delta(\mathbf{x}_1-\mathbf{x}_0)}{\mathrm{d}\Omega(\mathbf{x}_0)} + \right. \\ \left. 2\rho_0 \int_\Omega A(\mathbf{x}_1,\mathbf{x}_0) G(\mathbf{x},\mathbf{x}_0)\mathrm{d}\mathbf{x}_0 \right) Y(\mathbf{x},\mathbf{x}_1)\mathrm{d}\mathbf{x}. \quad (19)$$

Again, the equation can be written in discrete form as

$$\mathbf{A} = \mathbf{Y}\left(\mathbf{S} + 2\rho_0 \mathbf{G}^{\mathrm{s}}\mathbf{A}\right), \quad (20)$$

with $\mathbf{S} = \mathrm{diag}\left(\frac{1}{\mathrm{d}\Omega_i}\right)$ and the admittance matrix is given by

$$\mathbf{Y} = \mathbf{A}\left(\mathbf{S} + 2\rho_0 \mathbf{G}^{\mathrm{s}}\mathbf{A}\right)^{-1}. \quad (21)$$

Since $\mathbf{A}$ directly coincides with the acceleration matrix measured via impact testing, the admittance matrix can be expressed numerically. Once the admittance matrix is known, the total pressure on the surface can be calculated by evaluating (14) for an arbitrary incident pressure field.

3.4 Validation of the measurement method

In order to validate the results of the previous sections the estimated sound field above the plate absorber was compared with direct microphone measurements. The measurement setup is illustrated in Fig. 5.

The measurement was carried out in a semi-anechoic chamber with the plate absorber positioned on the reflective floor, in order to imitate baffling in an infinite rigid plane. The incident field was generated by a loudspeaker mounted on the top of the chamber 2 meters above the centre of the absorber. The total field was measured at the centre of the plate with a TMS 130P10 condenser microphone. To eliminate the effect of the loudspeaker response and undesired reflections the measurement was repeated without the absorber, with the result used as a correction reference spectrum.

The result of the measurement was compared with the estimated total field by evaluating (14) with the incident field assumed to be a vertical plane wave. The admittance matrix was calculated from the result of impact testing by (21), while the Green's matrix (12) was evaluated by using the NiHu MATLAB boundary element toolbox [10].

The result of comparison is depicted in Fig. 6, confirming the validity of the presented model. The figure suggests that the result of the numerical model coincides well with the microphone measurements in the frequency range of investigation, where the measurement geometry approximates fairly the baffled model. At frequencies higher than the depicted part of the spectrum significant discrepancies are present.

The qualitative investigation of Fig. 6 reveals that below the frequency range of the plate's modal behaviour the incident field is scattered rigidly from the surface (i.e. $P_{\mathrm{tot}} = 2$). In the range of modal behaviour mode shapes with nodal lines at the centre of the plate do not contribute significantly to the total pressure field, while other modes have severe effect on the resulting sound pressure. This result already shows that the locally reactive model, and the corresponding measurement procedures can not be used in the present geometry.

4. CALCULATION OF ABSORPTION CHARACTERISTICS

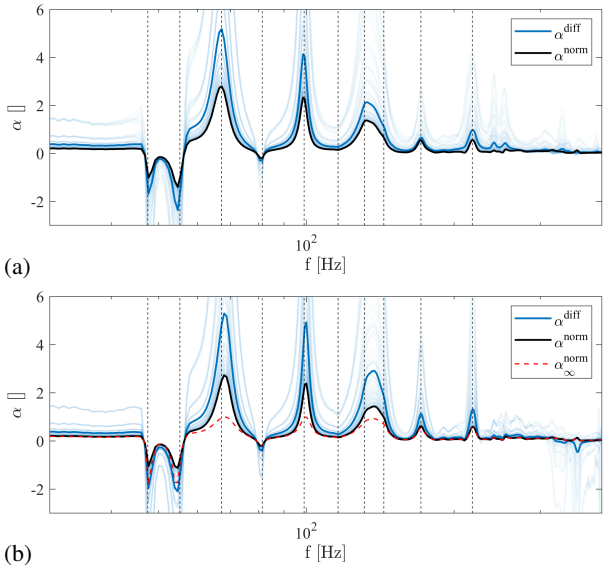

Figure 7. Estimated normal and statistical absorption coefficients from absorbed power estimation (a) and by using Thomasson's size correction with assuming locally reactive plate surface (b). Faded lines denote the individual directional absorption characteristics for different incdient angles.

Finally, the measurement based numerical model was used to estimate the absorption characteristics of the panel absorber.

The incident field was a plane wave arriving to the top plate at an elevation angle of θ and azimuth angle of ϕ, described by

$$P_{\text{in}}(\mathbf{x}) = \mathrm{e}^{-\mathrm{j}k(\cos\phi\sin\theta x + \sin\phi\sin\theta y)}. \tag{22}$$

As a straightforward estimation, the directional absorption coefficient of the sample can be defined as

$$\alpha(\theta,\phi) = \frac{\Pi_{\text{abs}}(\theta,\phi)}{\Pi_{\text{in}}(\theta)} = Z_0 \frac{\mathrm{Re}\left(\int_\Omega P_{\text{tot}}(\mathbf{x}) V^*_{\text{tot}}(\mathbf{x})\,\mathrm{d}\mathbf{x}\right)}{\cos\theta L_x L_y}, \tag{23}$$

with Π_{abs} and Π_{in} being the absorbed and incident power, L_x and L_y being the dimensions of the plate and $Z_0 = \rho_c c$ being the specific impedance of air (see eq. (12.30) in [8]). The diffuse field absorption coefficient of the plate absorber is calculated as

$$\alpha^{\text{diff}} = \frac{\int_0^{2\pi}\int_0^{\pi/2} \Pi_{\text{abs}}(\theta,\phi)\sin\theta \mathrm{d}\theta\,\mathrm{d}\phi}{\int_0^{2\pi}\int_0^{\pi/2} \Pi_{\text{in}}(\theta)\sin\theta \mathrm{d}\theta\,\mathrm{d}\phi}. \tag{24}$$

by averaging the absorbed and incident power over the possible incident directions.

The total pressure and total velocity over the surface were calculated numerically from (14) and (15) using the measured admittance matrix.

The diffuse and directional absorption coefficients are depicted in Fig. 7 (a), highlighting the absorption for a normal incident plane wave. The results suggest that instead of the intended plate-air (mass-spring) interaction the modal behaviour of the plate dominates the absorption characteristics of the entire layered structure: Even modes, for which the air cavity behind the plate act as an acoustic short-circuit re-radiate positive power into the half space, resulting in *negative* absorption coefficient. On the other hand, for odd modes the compressed air behind the plate can enter the porous absorber, therefore, the layered structure acts as a highly absorptive spring-mass system, leading to absorption coefficients *above unity*. This phenomena is even enhanced for lateral incident waves, with the incident pressure wave generating large plate vibrations at low incident intensities.

It is important to note that the apparent unphysical absorption factor exceeding unity reflects that on the plate's modal frequencies the absorber 'draws in' energy from surrounding regions due to a process of diffraction, therefore, the actual absorption area highly exceeds the plate's physical dimensions [11].

Finally the proposed extened reactive model was compared with a simplified approach introduced by Thomasson [3]. The model under discussion assumes a homogeneous, locally reactive impedance over the surface of the absorber given by Z_A, but includes size effects, by evaluating (23) analytically. The resulting directional absorption coefficient is given by

$$\alpha(\theta,\phi) = \frac{1}{\cos\theta}\frac{4\mathrm{Re}Z_A}{|Z_A + Z_R|^2}, \tag{25}$$

where Z_R is the normalized radiation impedance of the surface, calculated numerically as proposed in Appendix 12.A in [8]. In the present case the locally reacting impedance was calculated as

$$Z_A = \frac{1}{Z_0}\frac{\int_\Omega P_{\text{total}}(\mathbf{x})\mathrm{d}\mathbf{x}}{\int_\Omega V_{\text{total}}(\mathbf{x})\mathrm{d}\mathbf{x}}. \tag{26}$$

The resulting absorption characteristics are depicted in Fig. 7 (b). It is highlighted that the finite-sized locally reactive approach gives a limited approximation of the physical model proposed in the present paper.

Fig. 7 (b) also depicts the traditional absorption coefficient denoted by α_∞. In this limiting case the absorber surface assumed to be infinite with homogeneous surface impedance of Z_A, and with the radiation impedance being $Z_R = 1/\cos\theta$. With these assumptions the classic absorption formula is recovered

$$\alpha_\infty(\theta) = \frac{4\mathrm{Re}Z_A \cos\theta}{|Z_A \cos\theta + 1|^2}. \tag{27}$$

The surface impedance was obtained using (26). Fig. 7 (b) suggests that this locally reactive approximation – with no size-effect correction – gives only a qualitatively acceptable approximation for the physical based model while being maximized to unity. However, this formulation may be useful for describing the absorption of an infinite absorbing surface, on which the rectangular plate resonator is repeating periodically. This aspect is the subject of further investigation.

5. CONCLUSION

The present paper discussed a mechanical admittance-based measurement and modeling method allowing the coupling of vibrating planar surfaces into acoustical scattering simulations. The proposed approach was discussed in the context of predicting the sound absorbing properties of a small scale plate resonator exposed to incident plane waves, being a prominent example of a non-locally reacting surface.

The method relies on impact testing the resonator surface, resulting in high signal-to-noise ratio acceleration measurements. From the result of impact testing the surface's acoustic admittance function can be estimated by the numerical compensation of the re-radiated pressure field. Once the surface admittance is known the vibrating surface was coupled to numerical scattering simulations, allowing the estimation of the sound field properties over the absorber surface. These results may be used for predicting the sound absorption coefficient of the resonant absorber for an arbitrary incident pressure field. The validity of the presented formulations was verified by comparing numerical results with direct microphone measurements. Finally, the investigation of the currently measured plate absorber revealed that due to the small size of the absorber, instead of the intended characteristics, the absorption properties of the resonator are dominated by the modal behaviour of the top-plate.

6. ACKNOWLEDGMENTS

This work was supported by the OTKA PD-143129 grant, the János Bolyai Research Scholarship of the Hungarian Academy of Sciences, the ÚNKP-22-5-BME-318 New National Excellence Program of the Ministry for Innovation and Technology from the source of the National Research, Development and Innovation Fund and by ENTEL Engineering Research & Consulting Ltd., Hungary.

7. REFERENCES

[1] "ISO 354:2003," standard, International Organization for Standardization, Geneva, CH, 2003.

[2] "ISO 10534-2:1998," standard, International Organization for Standardization, Geneva, CH, 1998.

[3] S.-I. Thomasson, "On the absorption coefficient," *Acta Acoustica United with Acoustica*, vol. 44, no. 4, pp. 265–273, 1980.

[4] S.-I. Thomasson, "Theory and experiments on the sound absorption as function of the area," Tech. Rep. TRITA-TAK-8201, KTH Stockholm, 1982.

[5] H. Kuttruff, *Room Acoustics*. CRC Press, 2017.

[6] P. M. Morse and K. U. Ingard, *Theoretical Acoustics*. New York, NY: McGraw-Hill Book Company, 1st ed., 1968.

[7] E. G. Williams, *Fourier Acoustics: Sound Radiation and Nearfield Acoustical Holography*. London: Academic Press, 1st ed., 1999.

[8] J. Allard and N. Atalla, *Propagation of Sound in Porous Media: Modelling Sound Absorbing Materials*. Wiley, 2009.

[9] T. Cox and P. D'Antonio, *Acoustic Absorbers and Diffusers: Theory, Design and Application*. CRC Press, 2016.

[10] P. Fiala and P. Rucz, "Nihu: A multi-purpose open source fast multipole solver," in *Proceedings of DAGA2019*, (Rostock), DEGA, 2019.

[11] F. J. Fahy, *Sound Intensity*. Spon Press, 2nd edition ed.